Stress of Planet Gears with Thin Rims

Takeshi Ishida & Teruaki Hidaka
Yamaguchi University, Yamaguchi, Japan

Abstract

This article discusses the relationships among the fillet stress σ on a thin rim planet gear, the radial clearance between the gear rim and the gear shaft Δr, the tooth load P_n, the rim thickness h, the radius of curvature of the center line of the rim r, the face width b and the module m. It is shown theoretically that $P_n/(mb)$, $(h/r)(\Delta r/r)$ and $(h/m)(h/r)$ can express the tooth load, the radial clearance and the rim thickness, respectively. Furthermore, when the tooth loads are applied at the tips of a thin rim planet gear which is cut by a rack-type cutter with a pressure angle of 20° and a tip radius of 0.375 m, the maximum tensile and compressive stresses, by which both the amplitude and the mean value of the alte-rnating fillet stress can be estimated, are analyzed by the finite element method. They are expressed by equations using the expressions $P_n/(mb)$, $(h/r)(\Delta r/r)$, $(h/m)(h/r)$ and the number of teeth z.

Introduction

The fillet stress σ on a gear with a thick rim is proportional to the ratio of the tooth load to both the module and the face width, $P_n/(mb)$. Therefore, the fillet stress σ on the gear with a thick rim is frequently discussed when the ratio $P_n/(mb)$ is constant. The fillet stress on the gear with a thin rim is much different because of the elastic deformation of the rim (Refs. 1-6). The stress on the planet gear with a thin rim is influenced by the rim thickness and the radial clearance between the rim and the gear shaft (Refs. 3-6). Some dimensionless expressions have been used to show the relative rim thickness and the relative radial clearance. For the rim thickness, either the ratio of the rim thickness to the module *(h/m)* or the ratio of the rim thickness to the radius of curvature of the center line of the rim *(h/r)* is often used (Refs. 3-6). For the radial clearance, either the ratio of the radial clearance to the module $(\Delta r/m)$ or the ratio of the radial clearance to the radius of curvature of the center line of the rim $(\Delta r/r)$ is often used (Refs. 3-6). However, the effects of these ratios, *h/m*, *h/r*, $\Delta r/m$ and $\Delta r/r$, on the fillet stress have not been discussed sufficiently.

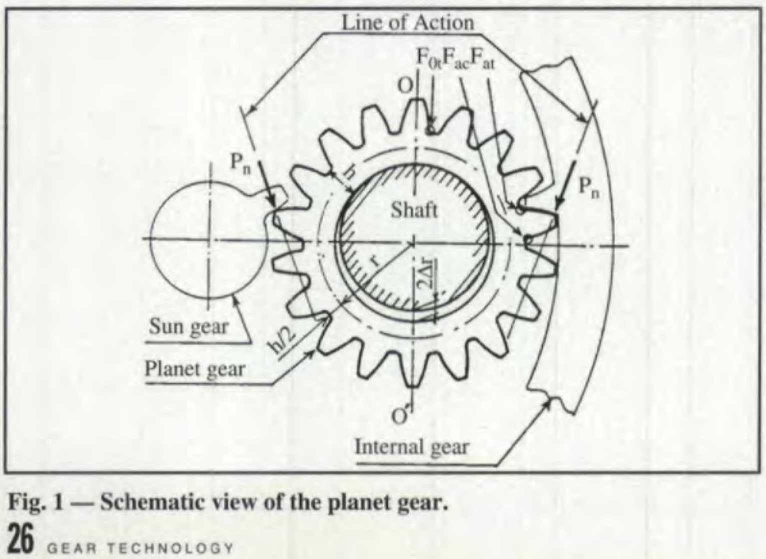

Fig. 1 — Schematic view of the planet gear.

This article discusses the relationships among the fillet stress σ, the radial clearance Δr, the tooth load P_n, the rim thickness h, the radius of curvature of the center line of the rim r, the face width b and the module m. It is shown in theory that $P_n/(mb)$ can express the tooth load, $(h/r)(\Delta r/r)$ can express the radial clearance, and $(h/m)(h/r)$ can express the rim thickness when the fillet stress is expressed by σ. In addition, the maximum stresses on the tension and compression side fillets of the loaded tooth, and the maximum stress on the fillet near the position where the rim receives the reaction force from the gear shaft are analyzed by the finite element method. Then the maximum stresses on those fillets, σ, (by which both the amplitude and the mean value of the alternating fillet stress can be estimated) are expressed with equations using the expressions $P_n/(mb)$, $(h/r)(\Delta r/r)$, $(h/m)(h/r)$ and the number of teeth z. This analysis is made in a particular case when tooth loads are applied at the tips of a thin rim planet gear which is cut by a rack-type cutter with a pressure angle of 20° and a tip radius of 0.375 m.

Planet Gears Discussed

Fig. 1 shows the schematic view of a planet gear with a radial clearance between the gear rim and the gear shaft. In the case of the planet gear, it has been shown that both the amplitude and the mean value of the alternating fillet stress can be estimated by using the maximum stresses on the tension and compression side fillets, shown by F_{at} and F_{ac} in Fig. 1, and the maximum stress on the fillet near the position where the reaction force is applied from the gear shaft, shown by F_{0t} in Fig. 1 (Ref. 4). Therefore, these three maximum stresses on F_{0t}, F_{at} and F_{ac} were analyzed in this study.

The pressure angle and the whole depth of the planet gears discussed were 20° and 2.25 m (m:module) respectively. The gears were assumed to be cut by a rack-type cutter with a tip radius of 0.375 m. Both the number of teeth and the rim thickness of the gears analyzed are shown in Table 1.

An example of the mesh pattern of the finite element model of the planet gear is shown in Fig. 2. The mesh pattern per one pitch of any planet gear model was almost the same as that shown in Fig. 2.

The longitudinal elastic modulus and the Poisson's ratio of the gears were assumed to be 206 GPa and 0.3, respectively. The gear shaft was assumed to be rigid because the contact stiffness between the planet gear rim and the gear shaft was considered to be much larger than the bending stiffness of the thin rim of the planet gear. The ratio of the tooth load to both the module and the face width, $P_n/(mb)$, was chosen as 124 N/mm^2.

Theoretical Discussion of Expressions of Fillet Stress, Tooth Load, Rim Thickness and Radial Clearance

Fillet stress on the loaded tooth of a thin rim planet gear with a large radial clearance must be approximately expressed as follows:

$$\sigma = \sigma_T + (\sigma_{Rb} + \sigma_{Ra}), \qquad (1)$$

Table 1 — Specifications of the planet gears discussed.

Number of teeth z	$(h/m)(h/r)$		
18	1.4 (0.2)	2.0 (0.3)	3.1 (0.5)
38	2.2 (0.13)	2.6 (0.16)	3.2 (0.19)
	4.0 (0.25)	4.9 (0.32)	
62	2.8 (0.1)	4.1 (0.15)	6.4 (0.24)
90	3.4 (0.08)	5.0 (0.12)	7.9 (0.2)

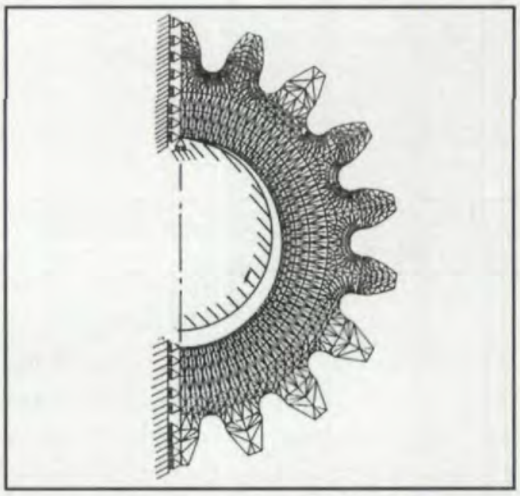

Fig. 2 — A mesh pattern of the planet gear model (z = 18, $(m/h)(r/h)$ = 0.645).

where σ_T shows the fillet stress of the loaded tooth when the effect of the rim stress is very small. σ_{Rb} and σ_{Ra} show the stresses caused by the bending moment of the rim and by the circumferential force of the rim, respectively. σ_T can be put as zero on the fillet of the tooth to which the tooth load is not applied. Since σ_{Rb} must be greater than σ_{Ra}, σ_{Ra} can be neglected in the case of the thin rim gear.

The distance to the center line of the rim from the intersection between the line of action and the center line of the tooth form is η. σ_{Rb} can be expressed as follows by using coefficients a_1 and a_2:

$$\sigma_{Rb} = a_1\{P_n r/(bh^2)\} + a_2\{P_n \eta/(bh^2)\}. \qquad (2)$$

In the case of a thin rim gear, the radius of curvature of the center line of the rim r is generally much larger than the distance η, i.e., $r >> \eta$. Eq. 2 can be rewritten as follows using $[P_n/(mb)]$, which is used in the case of the gear with a thin rim:

$$\sigma_{Rb} = a_1\{P_n/(mb)\}(m/h)(r/h). \qquad (3)$$

From Eq. 3, σ_{Rb} can be supposed to be approximately proportional to $(m/h)(r/h)$ when

Dr. Takeshi Ishida
has been an Associate Professor in the Department of Mechanical Engineering of Yamaguchi University since 1987.

Dr. Teruaki Hidaka
has been a Professor of Mechanical Engineering at Yamaguchi University since 1977.

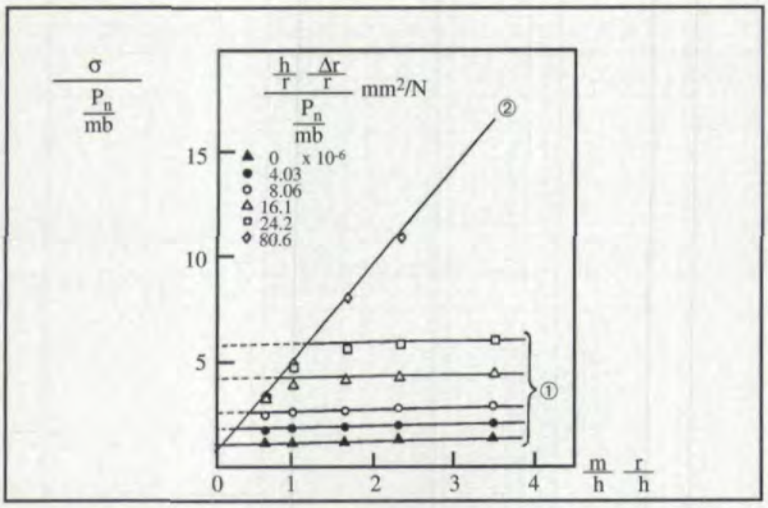

Fig. 3 — Relation between $\sigma_{at}/\{P_n/(mb)\}$ on F_{at} and $(m/h)(r/h)$ $(z = 38)$.

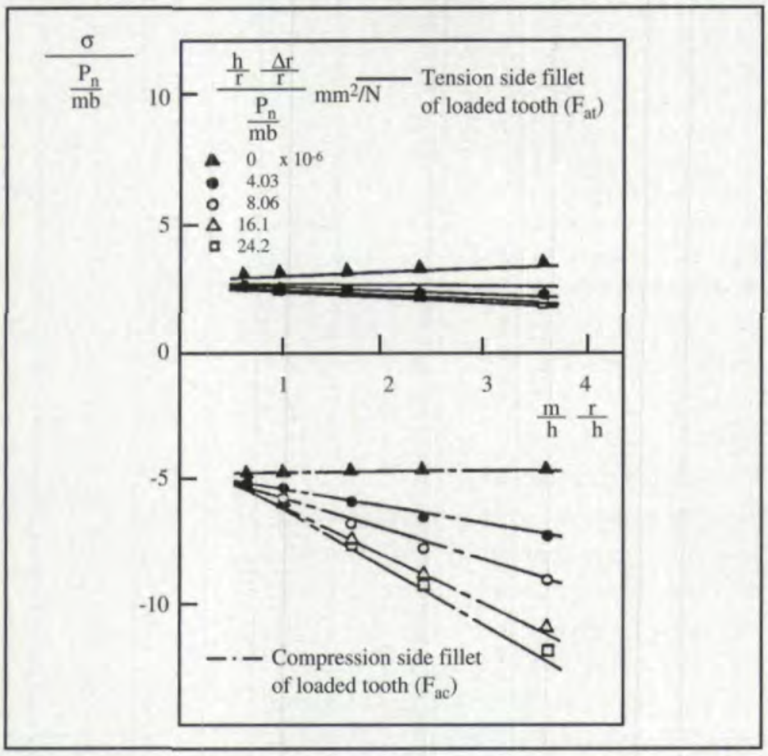

Fig. 4 — Relations between $\sigma_{at}/\{P_n/(mb)\}$ on F_{at} and $(m/h)(r/h)$, and between $\sigma_{ac}/\{P_n/(mb)\}$ on F_{ac} and $(m/h)(r/h)$ $(z = 38)$.

$[P_n/(mb)]$ is constant.

On the other hand, σ_T can be expressed by using the coefficient b_1 as follows:

$$\sigma_T = b_1(P_n/mb). \quad (4)$$

Therefore, Eq. 1 can be expressed approximately as follows:

$$\sigma = \{P_n/(mb)\}\{b_1 + a_1(m/h)(r/h)\} \quad (5)$$

When the radial clearance between the gear rim and the gear shaft decreases, the contact area between the gear rim and the gear shaft changes from line contact to face contact. Therefore, when discussing the fillet stresses on the planet gear with both a thin rim and a small radial clearance, the displacement of the gear rim must be considered.

The case where the radial clearance is very large and only line contact occurs is considered before the case of face contact. The displacement of the gear rim δ can be approximately expressed as follows because of $r >> \eta$:

$$\delta = c_1 P_n r^3/(bh^3) = c_1\{P_n/(mb)\}(m/h)(r/h)^2 r. \quad (6)$$

Then the following equation is reduced:

$$(h/r)(\delta/r) = c_1\{P_n/(mb)\}(m/h)(r/h). \quad (7)$$

Eq. 7 shows that when tooth loads are applied to any planet gear whose $(m/h)(r/h)$ are equal to one another under the condition where $P_n/(mb)$ is equal, $(h/r)(\delta/r)$ are the same, and the rim stress reaches σ_{Rb} as shown in Eq. 3. Therefore, when $(h/r)(\Delta r/r)$ is larger than $(h/r)(\delta/r)$, line contact between the rim and the gear shaft occurs, and the rim stress is proportional to $P_n/(mb)$.

Next, the case where $(h/r)(\Delta r/r)$ is less than $(h/r)(\delta/r)$ will be considered. On F_{0t} (shown in Fig. 1), as the radius of curvature of the rim changes from r to $(r - \Delta r)$, the following equation can be obtained:

$$1/(r - \Delta r) - 1/r = M/(EI), \quad (8)$$

where M, E and I denote the bending moment, the longitudinal elastic modulus and the moment of inertia of the cross section of the rim, respectively. Because $1/(r - \Delta r) - 1/r \approx \Delta r/r^2$ and M is proportional to σh^2, Eq. 8 becomes:

$$\sigma \text{ is proportional to } (h/r)(\Delta r/r). \quad (9)$$

It is clear from Eq. 9 that the fillet stress on F_{0t} is not a function of $(m/h)(r/h)$, but a function of $(h/r)(\Delta r/r)$. After the face contact between the rim and the gear shaft at the position near F_{0t}, face contact on other regions does not always occur. However, even in such cases, since $(h/r)(\delta/r)$ of the rim must be proportional to $(h/r)(\Delta r/r)$, the fillet stress in the region near which the face contact does not occur seems to be expressed by an equation similar to Eq. 5.

Approximate Expression of Maximum Fillet Stresses

Relation between the stress σ and $P_n/(mb)$. For planet gears whose number of teeth z and $(m/h)(r/h)$ are equal to each other, when $(h/r)(\Delta r/r)/\{P_n/(mb)\}$ is constant, the stress σ is proportional to $P_n/(mb)$ (Ref. 3). Therefore, in the case of the finite element analysis under $P_n/(mb)=124\ N/mm^2$, and denoting by $(h/r)(\Delta r/r)_{124}$ and σ_{124} the dimensionless radial clearance and the stress, respectively, when

$$(h/r)(\Delta r/r)/\{P_n/(mb)\} = (h/r)(\Delta r/r)_{124}/124 \quad (10)$$

is satisfied, the following equation must be satisfied.

$$\sigma/\{P_n/(mb)\} = \sigma_{124}/124 \quad (11)$$

Considering Eqs. 10 and 11, $(h/r)(\Delta r/r)_{124}/124$ and $\sigma_{124}/124$ are translated into $(h/r)(\Delta r/r)/\{P_n/(mb)\}$ and $\sigma/\{P_n/(mb)\}$ to express the approximate equations.

Relation between $\sigma/\{P_n/(mb)\}$ and $(m/h)(r/h)$. The relations between the maximum stresses on the fillets F_{0t}, F_{at} and F_{ac}, and $(m/h)(r/h)$ with a parameter $(h/r)(\Delta r/r)/\{P_n/(mb)\}$ were analyzed by the finite element method as shown in Figs. 3 and 4 where the number of teeth is $z = 38$. In Figs. 3 and 4, the stresses are translated into $\sigma/\{P_n/(mb)\}$. The relationship between $\sigma/\{P_n/(mb)\}$ and $(m/h)(r/h)$ with a parameter $(h/r)(\Delta r/r)/\{P_n/(mb)\}$, where the number of teeth are both $z = 18$ and 90, was also analyzed and shown in Figs. 5-8. Although the stresses on the planet gear with the number of teeth $z = 62$ were also analyzed, these results are not shown here. Symbols in Figs. 3-8 show the values analyzed by the finite element method, and the lines in Figs. 3-8 show the values obtained by the approximate equations mentioned below. The value of 80.6 x 10^{-6} mm^2/N for $(h/r)(\Delta r/r)/\{P_n/(mb)\}$ in Figs. 3, 5 and 7 corresponds to an extremely large radial clearance. It seems from these figures that the stress on F_{0t} when $(h/r)(\Delta r/r)/\{P_n/(mb)\}$ = 80.8 x 10^{-6} mm²/N is proportional to $(m/h)(r/h)$. This phenomenon must correspond to Eq. 3. Moreover, although Eq. 9 shows that the stress on F_{0t} when $(h/r)(\Delta r/r)/\{P_n/(mb)\}$ =80.8 x 10^{-6} mm^2/N does not change with $(m/h)(r/h)$, the stress changes slightly with $(m/h)(r/h)$ in Figs. 3, 5 and 7 owing to the circumferential force of the rim. Because it is clear from Figs. 3-8 that the relations between $\sigma/\{P_n/(mb)\}$ and $(m/h)(r/h)$ on each fillet can be approximately expressed by straight lines, the relation between $\sigma/\{P_n/(mb)\}$ and $(m/h)(r/h)$ is expressed as follows:

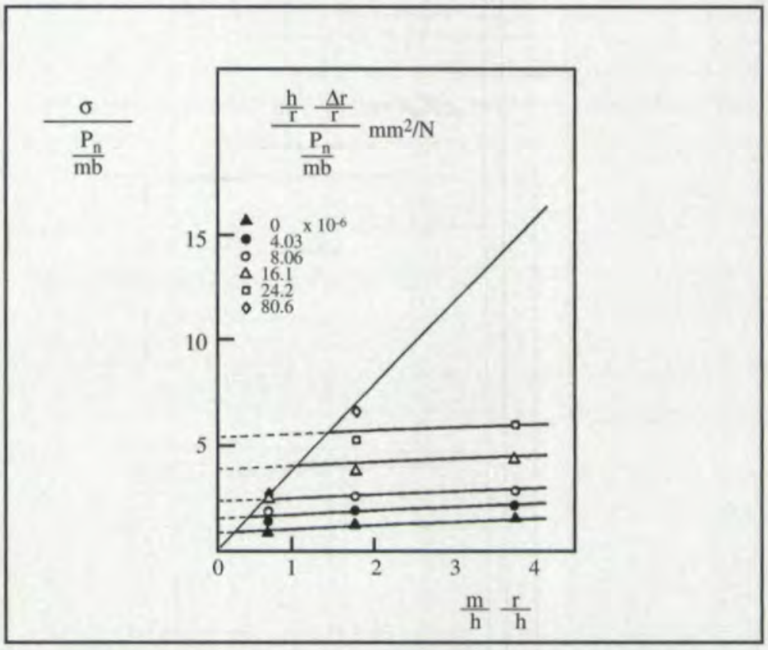

Fig. 5 — Relation between $\sigma_{at}/\{P_n/(mb)\}$ on F_{at} and $(m/h)(r/h)$ (z = 18).

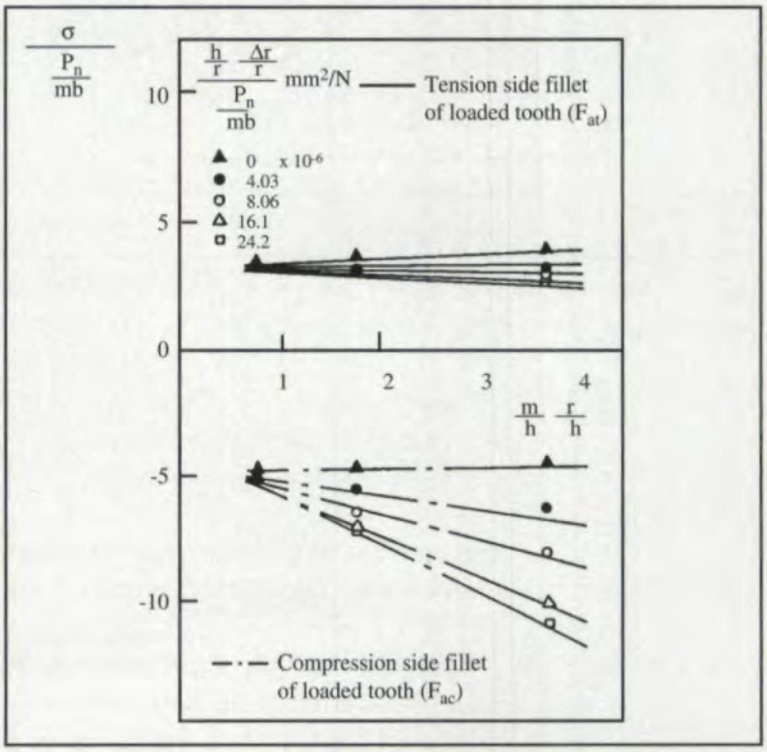

Fig. 6 — Relations between $\sigma_{at}/\{P_n/(mb)\}$ on F_{at} and $(m/h)(r/h)$, and between $\sigma_{ac}/\{P_n/(mb)\}$ on F_{ac} and $(m/h)(r/h)$ (z = 18).

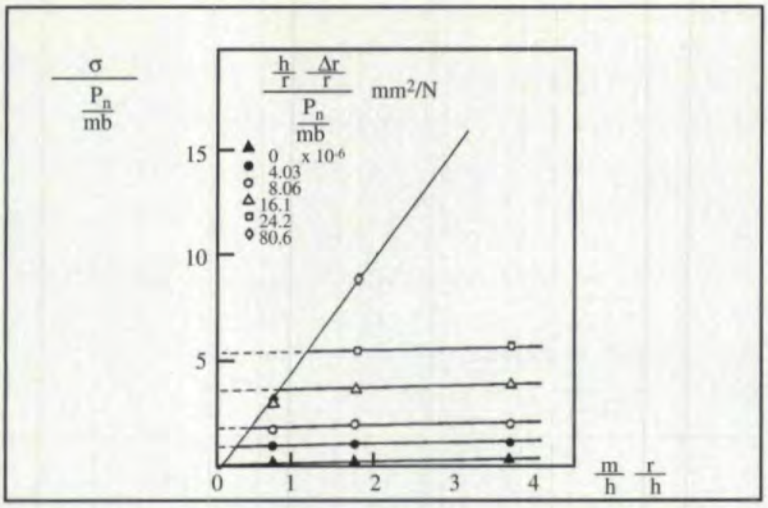

Fig. 7 — Relation between $\sigma_{at}/\{P_n/(mb)\}$ on F_{at} and $(m/h)(r/h)$ ($z = 90$).

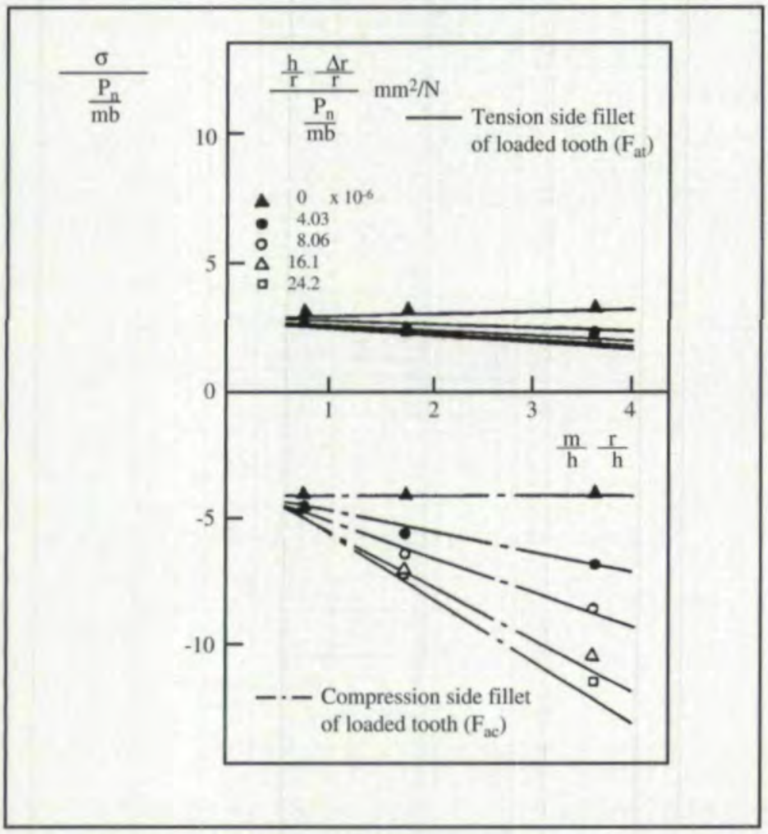

Fig. 8 — Relations between $\sigma_{at}/\{P_n/(mb)\}$ on F_{at} and $(m/h)(r/h)$, and between $\sigma_{ac}/\{P_n/(mb)\}$ on F_{ac} and $(m/h)(r/h)$ ($z = 90$).

$$\sigma_{0t}/\{P_n/(mb)\} = A_{0t}(m/h)(r/h) + B_{0t}, \quad (12)$$
$$\sigma_{at}/\{P_n/(mb)\} = A_{at}(m/h)(r/h) + B_{at},$$
$$\sigma_{ac}/\{P_n/(mb)\} = A_{ac}(m/h)(r/h) + B_{ac},$$

where A and B denote the coefficients influenced by the number of teeth z and $(h/r)(\Delta r/r)/\{P_n/(mb)\}$.

$\sigma_{0t}/\{P_n/(mb)\}$ on fillet F_{0t}. Considering the result shown in Fig. 3, the relation between $\sigma_{0t}/\{P_n/(mb)\}$ and $(m/h)(r/h)$ can be expressed approximately by two kinds of lines as shown by **1** and **2** in Fig. 3. The values due to **1** and **2** are shown by σ_{0t1} and σ_{0t2}, respectively. Then comparing σ_{0t1} and σ_{0t2}, the values shown by the solid lines are chosen as σ_{0t}. Fig. 9 shows the relationship between $\sigma/\{P_n/(mb)\}$ and $(h/r)(\Delta r/r)/\{P_n/(mb)\}$ when the number of teeth $z = 18$ and $(m/h)(r/h) = 1.69$. As shown in Fig. 9, when $(h/r)(\Delta r/r)/\{P_n/(mb)\}$ is small, $\sigma_{0t1}/\{P_n/(mb)\}$ increases linearly before reaching the constant value of $\sigma_{0t2}/\{P_n/(mb)\}$. This corresponds to Eq. 9. Therefore, when $(h/r)(\Delta r/r)/\{P_n/(mb)\}$ is small (before $\sigma_{0t1}/\{P_n/(mb)\}$ reaches the constant value), the coefficients A_{0t1} and B_{0t1} in Eq. 10 can be approximated as follows:

$$A_{0t1} = a_{0t11}(z)(h/r)(\Delta r/r)/\{P_n/(mb)\} + a_{0t12}(z),$$
$$B_{0t1} = b_{0t11}(z)(h/r)(\Delta r/r)/\{P_n/(mb)\} + b_{0t12}(z), \quad (13)$$

where the coefficients a and b are the function of the number of teeth z. Because the coefficient A_{0t1} hardly changes with $(h/r)(\Delta r/r)/\{P_n/(mb)\}$, and is almost constant, $a_{0t11} \approx 0$ is reduced under the condition when z is constant. When $(h/r)(\Delta r/r)/\{P_n/(mb)\}$ is large (after $\sigma_{0t1}/\{P_n/(mb)\}$ reaches the constant value in Fig. 3), because $\sigma_{0t}/\{P_n/(mb)\}$ is approximately proportional to $(m/h)(r/h)$ and is not a function of $(h/r)(\Delta r/r)/\{P_n/(mb)\}$, coefficients A_{0t2} and B_{0t2} are reduced as follows:

$$A_{0t2} = a_{0t22}(z)$$
$$B_{0t2} = 0 \quad (14)$$

Analyzing the results shown in Figs. 3-8, the relations between coefficients A_{0t1}, B_{0t1}, A_{0t2} and B_{0t2} and $(h/r)(\Delta r/r)/\{P_n/(mb)\}$ respectively, coefficients a and b are determined as shown in Table 2.

$\sigma_{at}/\{P_n/(mb)\}$ and $\sigma_{ac}/\{P_n/(mb)\}$ on fillets F_{at} and F_{ac}. It seems from Fig. 9 that coefficients A_{at}, B_{at}, A_{ac} and B_{ac} can be expressed by exponential functions of $(h/r)(\Delta r/r)/\{P_n/(mb)\}$. However, discussing the effects of $(h/r)(\Delta r/r)/\{P_n/(mb)\}$ on the coefficients A_{at}, B_{at}, A_{ac} and B_{ac}, it was concluded that the first degree equations of $(h/r)(\Delta r/r)/\{P_n/(mb)\}$ were enough to express both B_{at} and B_{ac}. Therefore, the approximate equations to express the coefficients A_{at}, B_{at}, A_{ac} and B_{ac} were chosen as follows:

$$A_{at} = a_{at1} + a_{at2}\exp\{a_{at3}(h/r)(\Delta r/r)/\{P_n/(mb)\}$$

$$B_{at} = b_{at1}(h/r)(r/r)/\{P_n/(mb)\} + b_{at2}$$
$$A_{ac} = a_{ac1} + a_{ac2}\exp\{a_{ac3}(h/r)(\Delta r/r)/\{P_n/(mb)\}$$
$$B_{ac} = b_{ac1}(h/r)(\Delta r/r)/\{P_n/(mb)\} + b_{ac2} \quad (15)$$

The coefficients *a* and *b* are shown in Table 2.

Comparison between approximated value and value by finite element method. The values calculated by the approximate Eqs. 12-15 are shown by the solid lines and the dotted lines in Figs. 3-8. It is clear from Figs. 3-8 that the approximate values on the fillets are almost the same as the values obtained by the finite element method. Although the comparison in the case where the number of teeth is $z = 62$ is not shown here, the approximate values were again almost the same as the values obtained by the finite element method.

Approximation of Mean Value and Amplitude of Alternating Fillet Stress

Comparing σ_{0t} calculated by Eqs. 12-14 with σ_{at} calculated by Eqs 12 and 15, the larger value is chosen as σ_t. Using σ_t and $\sigma_c = \sigma_{ac}$, both the mean value σ_m and the amplitude σ_r of the alternating fillet stress on the weakest section of the planet gear can be calculated as follows (Ref. 4):

$$\sigma_m = (\sigma_t + \sigma_c)/2$$
$$\sigma_r = (\sigma_t - \sigma_c)/2 \quad (16)$$

Summary

In order to estimate the bending strength of a spur planet gear with a thin rim whose pressure angle is 20° and whole depth is 2.25 m, the maximum stresses on both the tension side and compression side fillets of the loaded tooth, and the maximum stress on the fillet near the position where the reaction force from the gear shaft is applied, were analyzed by the finite element method, and were expressed by approximate equations. ■

Acknowledgement: *This article appeared in Italian in* Organi di Trasmissione, *published by Techniche Nuove S. p. A., Milan, Italy. Reprinted with permission.*

References:

1. Hidaka, T., Ishida, T. and Uchida, F. *Bulletin of JSME.* Vol. 27, No. 223 (1984), pp. 110-116.
2. Hidaka, T., Ishida, T. and Uchida, F. *Bulletin of JSME.* Vol. 28, No. 236 (1985), pp. 329-336.
3. Ishida, T., Hidaka, T. and Takizawa, H. *Bulletin of JSME.* Vol. 28, No. 241 (1985), pp. 1505-1511.
4. Ishida, T., Hidaka, T. and Takizawa, H. *Bulletin of JSME.* Vol. 28, No. 244 (1985), pp. 2422-2428.

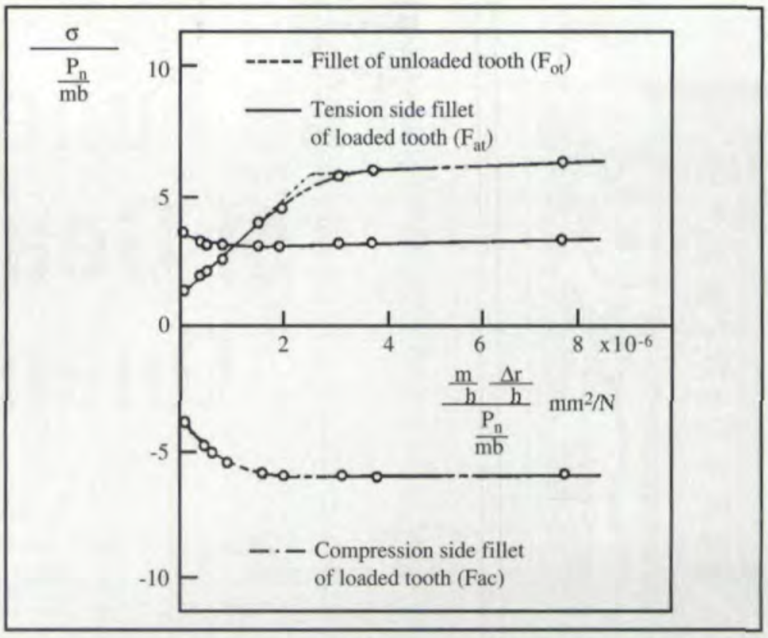

Fig. 9 — Relation between $\sigma/\{P_n/(mb)\}$ and $(h/r)(\Delta r/r)/\{P_n/(mb)\}$ on each fillet [$z = 18$, $(m/h)(r/h) = 1.69$].

Table 2 — Coefficients for the approximate Equations 12 - 15.

A_{0t1}	a_{0t11}	0
	a_{0t12}	2.72/z + 0.0677
B_{0t1}	b_{0t11}	1000(-777/z + 231)
	b_{0t12}	11.3/z + 0.119
A_{0t2}	a_{0t11}	0
	a_{0t12}	-26.3/z + 5.63
B_{0t2}	0	
A_{at}	a_{at1}	-0.645/z - 0.242
	a_{at2}	2.48/z + 0.297
	a_{at3}	10000(377/z - 30.3)
B_{at}	b_{at1}	1000(317/z - 15.1)
	b_{at2}	9.68/z + 2.97
A_{ac}	a_{ac1}	11.8/z - 3.06
	a_{ac2}	-11.2/z + 3.03
	a_{ac3}	-78200
B_{ac}	b_{ac1}	36000
	b_{ac2}	-14.8/z - 3.89

5. Oda, S., Miyachika, K. and Takeda, A. *Trans. Jpn. Soc. Mech. Eng., C* (in Japanese), Vol. 49, No. 445 (1983), pp. 1538-1544.
6. Oda, S., Miyachika, K. and Oka, H. *Trans. Jpn. Soc. Mech. Eng., C* (in Japanese), Vol. 52, No. 479 (1986), pp. 1972-1978.